Hadron Therapy: Radiotherapy Using Fast Ion Beams

Oliver Jäkel*

German Cancer Research Center
Department for Medical Physics in Radiation Oncology
Im Neuenheimer Feld 280, 69120 Heidelberg, Germany

Abstract

Charged particle beams offer an improved dose conformation to the target volume as compared to photon radiotherapy, with better sparing of normal tissue structures close to the target. In addition, beams of ions heavier than helium exhibit a strong increase of the LET in the Bragg peak as compared to the entrance region. These physical and biological properties make ion beams more favorable for radiation therapy of cancer than photon beams. As a consequence particle therapy with protons and heavy ions has gained increasing interest worldwide.

This contribution summarizes the physical and biological principles of charged particle therapy with ion beams and highlights some of the developments in the field of beam delivery and beam monitoring for a scanned ion beam, as well as the principles of treatment planning and the determination of absorbed dose in ion beams. The clinical experience gathered so far with carbon ion therapy is briefly reviewed.

Contents

* E-mail: o.jaekel@dkfz.de

1. Introduction: Status of Ion Therapy in 2006

In 2004, radiation therapy with hadron beams celebrated its 50th anniversary. The proposal to use heavy charged particles in radiation medicine dates back to 1946, when Dr. Robert R. Wilson, a physicist who had worked on developing particle accelerators, was the first to propose the use of protons for cancer therapy (Wilson, 1946). Less than 10 years later, in 1954 protons were used to treat cancer patients for the first time in Berkeley and in 1957 also helium ions were used at the same facility (Sisterson, 2005). In the 70s, heavier ions, like neon, silicon and argon were introduced for cancer therapy also at the Lawrence Berkeley Laboratory and many encouraging results (esp. in skull base tumors and paraspinal tumors) were achieved (Castro et al., 1994; Castro, 1997).

Today, particle therapy with protons and carbon ions has gained increasing interest. Worldwide, there are about 25 therapy units for treating patients with protons. The majority of the particle therapy centers are located in physics research laboratories, and only a few centers are available in a hospital environment. This situation is currently changing: There are more then 20 centers under construction or in the planning phase which will start to treat patients within the next 5 years (Sisterson, 2005), and nearly all those future installations will be hospital based. Obviously, the time has come that particle therapy is merging into clinics.

The availability of heavy ion RT is currently limited, as worldwide only 3 facilities offer carbon ion RT: two hospital based facilities in Japan (HIMAC/Chiba and HIBMC/Hyogo) and a physics research facility at GSI, Darmstadt in Germany. There is, however, an increasing interest in ion radiotherapy especially in Europe, where new facilities are being built in Germany (Heeg et al., 2004) and Italy (Amaldi, 2004) or are in an advanced planning phase like in Austria, France and Sweden (Sisterson, 2005).

This contribution gives an overview on the physical and biological background and of some of the physics problems connected to the use of heavy charged particles in cancer therapy.

2. Physical Properties of Ion Beams

As the physical and biological properties of proton beams differ significantly from beams of heavier particles, there is a distinction between the two categories "proton-therapy", characterized by low linear energy transfer (LET) and "heavy-ion therapy", with high LET properties.

Charged particles passing through tissue slow down losing energy in atomic interactions. This reduces the energy of the particles, which in turn causes increased energy loss, reaching a maximum at the end of range and causing the maximum dose deposition within the target area. In addition, due to nuclear interactions the number of primary particles is reduced and light fragments are produced. The primary rationale for radiotherapy with heavy charged particles is this sharp increase of dose in a well defined depth (Bragg peak) and the rapid dose fall-off beyond that maximum (Figure 1).

Mono-energetic Bragg peaks are usually not wide enough to cover most treatment volumes. By superimposing a set of beams with decreasing energies and weights, a "Spread out Break Peak" (SOBP) is generated, which delivers the desired dose to the whole treatment volume (Figure 1).

The ratio of Bragg peak dose *versus* dose in the entrance region is larger for heavy ions than for protons. Due to their larger mass, angular and energy straggling becomes negligible for heavy ions as compared to protons. Heavy ions therefore offer an improved dose conformation as compared to photon and proton RT, with better sparing of normal tissue structures close to the target.

The possibility to concentrate the radiation dose to the tumor while sparing the surrounding normal tissue is called dose conformation. The rational for the development of conformal radiation therapy techniques is found in radiobiology. The probability to control the growth of a tumor is increasing with the delivered dose. The same is true, however, for the probability of radiation related side effects

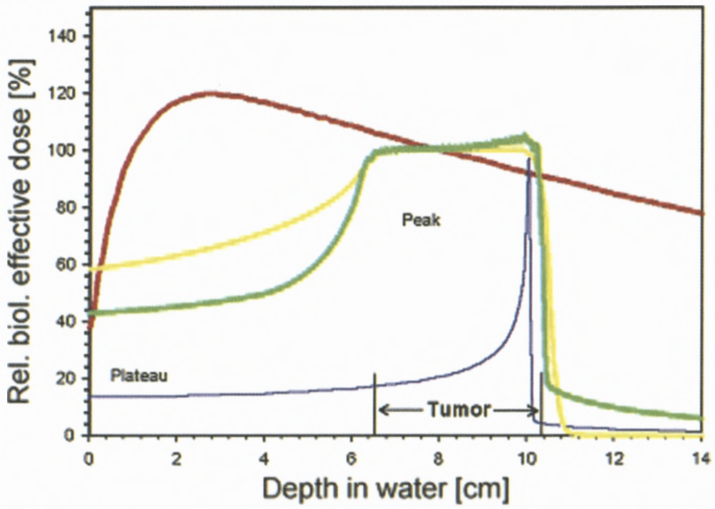

Figure 1. Biologically effective dose, as a function of the penetration depth in water, for high energy photon beams (red line), a mono-energetic carbon ion Bragg peak (blue line) and spread-out Bragg peaks of protons (yellow line) and carbon ions (green line). The given numbers are relative units, normalized to dose at 8 cm depth. For photons the biologically effective dose is equivalent to the absorbed dose, while for protons a constant RBE of 1.1 is assumed. The RBE for carbon was calculated using the track structure model by Scholz (see text).

in normal tissue. In many clinical cases, the dose that can be delivered to a tumor (and hence the tumor control) is limited by the radiation tolerance of the surrounding normal tissue. It has been observed, however, that the radiation tolerance of many organs is increasing if the irradiated volume of that organ is decreased (the so-called dose-volume effect). Consequently, if the irradiated volume of normal tissue can be minimized by conformal radiation therapy, a higher dose can be delivered to the tumor and thus a better outcome can be achieved without increasing the risk of side effects. This effect is the basis of most developments in the field of radiation therapy in the last decades. The highest degree of dose conformation can currently be achieved with proton and ion beams.

Ion beams undergo nuclear fragmentation processes during their passage through tissue. Most energetic fragments are produced in the projectile fragmentation (resulting in a spectrum of proton, helium, lithium, beryllium, boron and carbon ions for a primary carbon beam), while the fragmentation of target nuclei plays only a minor role. Monte Carlo transport simulations show, that when a beam of 290 MeV/u carbon ions penetrates into a depth in water of 15 cm, only about 40% of the primary ions reach the Bragg peak and only about 43% of

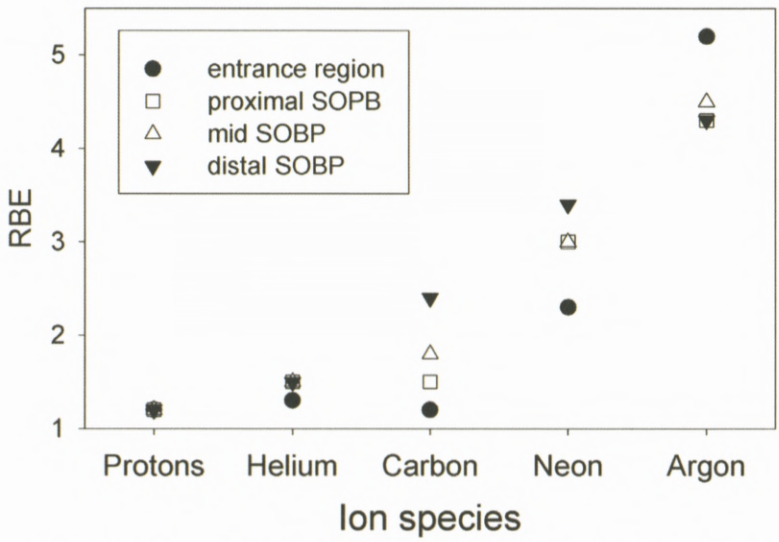

Figure 2. Relative biological effectiveness for crypt cells of mice after irradiation with ions in different positions of the spread-out Bragg peak (SOBP). The modulation depth of the SOBP was 8–10 cm, the initial beam energy was 160, 225, 400, 557 and 570 MeV/u for p, He, C, Ne and Ar ions, respectively. Figure reprinted from Jäkel (2006).

the total beam energy is deposited by carbon ions (Geithner et al., 2006). About 50% of the initial energy is transferred to lighter fragments and neutrons and the remainder is spent into gammas and nuclear binding energies.

The resulting complex radiation spectrum is of importance for the understanding of the biological effects of ion beams, but also to model the response of radiation detectors, like ionization chambers, thermo-luminescence detectors or even radiochromic film response. Modeling of these nuclear fragmentation effects is therefore an important problem in the application of ion beams in cancer therapy.

3. Radiobiological Properties of Ion Beams

In addition to the dose conformation, heavy ions exhibit a strong increase of the linear energy transfer (LET) in the Bragg peak as compared to the entrance region. The radiobiological advantage of high LET radiation in tumor therapy is well known from neutron therapy. Unlike in radiotherapy with neutron beams, in heavy ion radiotherapy the high LET region can be conformed to the tumor. The increasing biological effectiveness of ions with larger charge is shown in Figure 2.

While helium ions are very similar to protons in their biological properties, carbon or neon ions exhibit an increased relative biological effectiveness (RBE) in the Bragg peak as compared to the entrance region (see Figure 2). The RBE ratio (Bragg peak *versus* entrance region) is highest for carbon ions. For ions heavier than neon, the RBE in the entrance region is even higher than in the Bragg peak (like for argon).

Another disadvantage of heavy ions for radiotherapy is the increase of nuclear fragmentation processes, which leads to a fragment tail in the depth dose distribution that extends beyond the Bragg peak (see Figure 1).

The higher biological effectiveness of high LET radiation as compared to low LET radiation can be modeled by so-called track-structure models (Scholz and Kraft, 1994, 1997). According to these models the basic difference of high and low LET radiation, is the high local dose that is deposited close to the primary particle track of a high LET particle. If one assumes that the nonlinear relation between cell survival and dose can be applied also for subvolumes of a cell nucleus (where "lethal events" in the cell nucleus are considered) it becomes clear, that the integral effect for the cell nucleus is dependent on the pattern of the local dose distribution: irradiation of small subvolumes with a high dose is more effective than a homogeneous dose over the whole nucleus (keeping the average dose constant). If assumptions on the local radial dose distributions are made, this can be used to extract the relative biological effectiveness for ions beams from known survival data for cells after low LET irradiation.

It should be noted that besides the larger effect in cell killing, there are some more radiobiological effects, which make heavier ions beneficial for tumor therapy. It is known e.g., that for low LET radiation the survival of cells depends critically on the oxygen saturation of tissue. This is due to the production of oxygen radicals in the cell due to radiation. Many solid tumors, which exhibit hypoxic areas are therefore very resistant to low LET radiation. For high LET radiation, it is known, that the oxygen saturation of tissue plays only a minor role. High LET particles should therefore be especially useful in the treatment of radio-resistant tumors. There is also a smaller variation in the sensitivity of cells in different parts of the cell cycle when using high LET radiation instead of low LET radiation.

4. Clinical Results Obtained with Ion Beams

Since the availability of ion beams is still limited, there is only very little clinical experience with ion beams, especially, when ions heavier than Helium are considered. In 2006 roughly 2500 patients have been treated worldwide with carbon

ions. About 2000 patients were treated at the Japanese heavy ion facility HIMAC, which has been in operation since 1994.

At HIMAC a number of studies are ongoing using ion RT for the treatment of tumors of the head and neck, prostate, lung, liver as well as sarcomas of soft tissue and bone and uterine carcinomas. A report on the clinical results is found in Tsujii et al. (2004).

The fractionation scheme used is generally 16 fractions in 4 weeks for head and neck tumors as well as for sarcomas of bone and soft tissue. It was significantly shortened for lung cancer (9 fractions in 3 weeks) and liver tumors (12 fractions in 3 weeks) and is being further shortened to 4 fractions in 1 week for both indications. The latest results are from dose escalation studies in lung tumors and soft tissue sarcoma.

In two phase I/II trials non-small cell lung cancer (NSCLC), using different fractionation schemes (18 fractions in 6 weeks and 9 fractions in 3 weeks), a dose escalation was performed from 59.4 to 94.5 Gye[1] and from 68.4 to 79.2 Gye, respectively (Miyamoto et al., 2003; Koto, 2004). The resulting overall control rates for the 6- and 3-week fractionation were 64% and 84%, respectively. The total recurrence rate was 23.2%.

For unresectable bone and soft tissue sarcomas, a further phase I/II trial was performed with doses between 52.8 to 73.6 Gye (Kamada et al., 2002), applied in 16 fractions over 4 weeks. The observed overall control rates were 88% and 73% at 1 year and 3 years, respectively.

At GSI, about 300 patients have been treated with carbon ions since 1997. An overview over the results is found in Schulz-Ertner et al. (2004). The majority of patients was treated for skull base tumors. The median dose was 60 Gye (20 fractions each 3 Gye). The 3-year overall local control rate was 91%. The observed side effects were only very moderate (Schulz-Ertner et al., 2002).

Figure 3 shows an example of a treatment plan for patient with a chondrosarcoma close to the brain stem treated with carbon ions at GSI. The excellent dose conformation of the 90% isodose to the target is clearly demonstrated, although only two horizontal treatment fields were used here. The dose sparing of the relevant organs at risk can also be seen in the dose distribution.

Another group of patients was treated at GSI for a malignant salivary gland tumor (adenoid cystic carcinoma) using a combination of photon therapy and a carbon ion boost. The carbon therapy is given only to the macroscopic tumor residual (dose 18 Gye), while the photon dose is given to a much larger volume.

An analysis showed an actuarial local control rate of 62% at 3 years can be achieved, while in patients treated with photons alone, only 25% control rate could

[1] Gye stands for "Gray equivalent" and is commonly used to specify biologically effective dose.

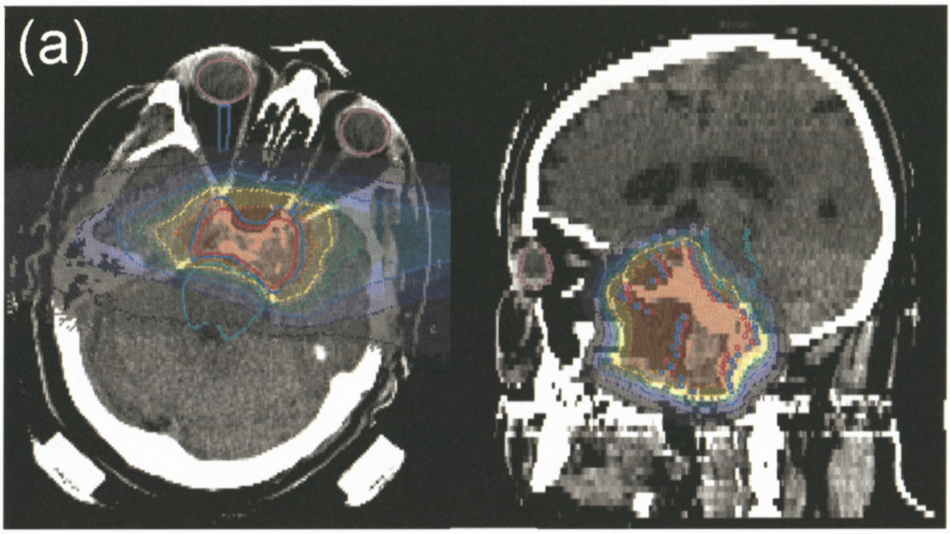

Figure 3. Example of a treatment plan for fully fractionated radiotherapy using 2 nearly opposing fields of carbon ions. The dose distribution at isodoses of 10%, 30%, 50%, 70% and 90% of the total dose (60 Gye) is shown, respectively. The colored lines indicate the primary and secondary target volume (red, blue), the brain stem (green line), optical nerves (blue) and eyes (pink), respectively.

be achieved (Schulz-Ertner et al., 2003). Again, severe side effects were observed only in few patients.

5. Beam Application and Beam Diagnostics

There exist two principal methods to shape the beam and thus to tailor the dose to the target volume, which will be described in the next section.

Passive beam delivery techniques (Figure 4a) use double-scattering systems or wobbling-magnets in combination with scatterers to produce large particle fields (Kanai, 1999). The particle field is then confined to the tumor cross-section by individually manufactured collimators or multi-leaf-collimators. To generate the SOBP, a rotating modulator wheel is inserted into the beam. This device introduces periodically material of varying thickness into the beam which results in a periodical modulation of the range. Alternatively, a static filter of varying thickness may be applied. This so-called ridge-filter uses lateral scattering to produce a homogeneous range modulation over the lateral extension of the treatment field. Each modulator-wheel or ridge filter is connected to a specific SOBP and is selected according to the extension of the tumor in depth. To adjust the SOBP to the distal edge of the tumor, range shifters are used. Finally, compensators

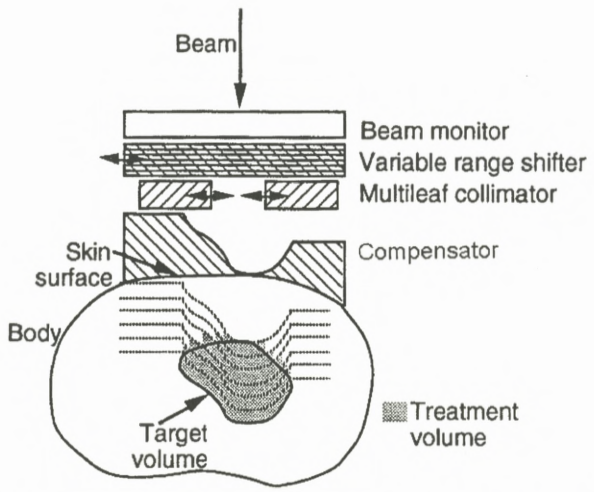

Figure 4a. Principle of the passive dose delivery. Shown is the incoming broadened beam that is modulated in depth. The range shifter shifts the SOBP to the desired depth, while collimator and compensator are patient specific devices. The lines in the body represent the distal dose fall-off that can be shifted in depth with the range shifter. Figure reproduced from Jäkel (2006).

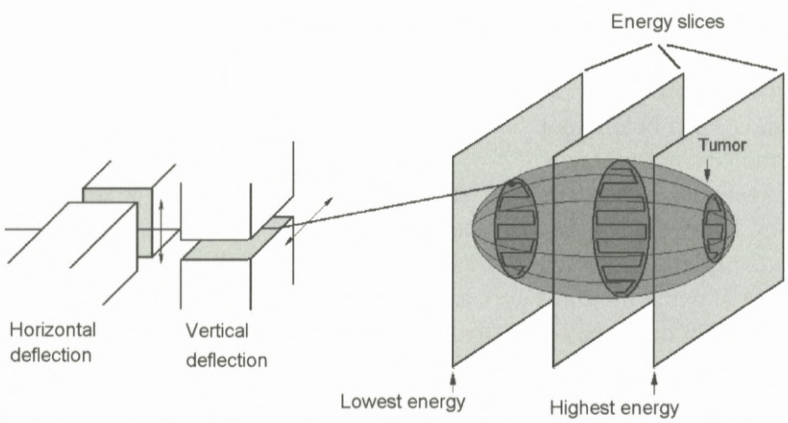

Figure 4b. Principle of an active beam delivery: a mono-energetic pencil beam is scanned over the tumour cross section. After one slice is irradiated the energy of the beam extracted from the synchrotron can be switched to the next energy.

manufactured for the individual field of each patient can be used to adjust the dose distribution to the distal edge of the tumor. As the extension of the SOBP remains constant over the tumor cross-section, the dose conformation at the distal edge is connected to high doses in the normal tissue at the proximal edge of the tumor (Figure 4a).

Another way of beam delivery is called active beam shaping (Haberer et al., 1993). This system takes advantage of the electric charge of the particles, in order to produce a tightly focused pencil beam that is then deflected laterally by two magnetic dipoles to allow a scanning of the beam over the treatment field. When the beam is produced with a synchrotron, the energy can be switched from pulse to pulse in order to adapt the range of the particles in tissue. This way, a target volume can be scanned in three dimensions and the dose distribution can be tailored to any irregular shape without any passive absorbers or patient specific devices, like compensators or collimators. Therefore, the high dose region can also be conformed to the proximal end of the target volume and the integral dose as well as the non-target volume receiving high LET radiation is minimized. Figure 4b shows the principle of the active beam delivery system.

There is only one facility (GSI) where beam scanning for carbon ions is already applied clinically. The GSI beam delivery system allows for a 3D scanning of arbitrarily shaped volumes with a spatial resolution of 1mm in all three directions. Typically, a beam width of 3–10 mm full-width half-maximum is scanned over a regular grid of points with typically 2–3 mm spacing. The accelerator energy can be switched from pulse to pulse and the energy can be selected from a library of 252 accelerator energies.

An essential prerequisite for such a beam scanning system is a suitable beam diagnostic system that is capable of monitoring the exact position and intensity of the beam at each beam spot. The monitoring system is connected via a feedback loop to the scanner magnets.

The system designed at GSI, relies on three large area ionization chambers (18 cm by 18 cm size of the active area) for the intensity measurement. Two chambers are completely identical in their design and readout, (using a chamber gas of Argon:CO_2), while the third uses a different electronic system (and air filling), in order to have redundancy and diversity built into the system. The resolution of the chambers in terms of particle number is around 1000 particles per sampling interval (which reflects an accuracy of about 1% in dose). The sampling interval is around 12 μs, in order to allow for a number of measurements at each beam position.

The intensity monitors are calibrated in terms of particle number and are used to switch the beam via the feedback loop to the next scan point if a predefined par-

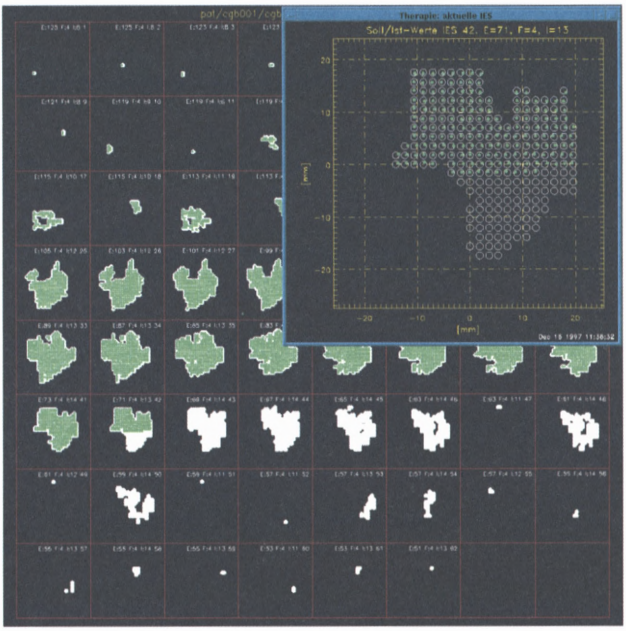

Figure 5. Screenshot of the therapy online monitor (TOM) developed at GSI. It displays the measured data on the actual position of the beam and indicates if the correct particle number was delivered by varying colors. The data from the monitoring system are displayed nearly in real-time.

ticle number for a given scan point has been reached. The chambers are operated at a high voltage which yields a charge collection efficiency of 99.5%.

For detection of the beam position, two additional large area multi wire proportional chambers are installed. They are made up of two wire planes with 112 wires with a spacing of 2 mm. This allows a determination of the beam position with a spatial resolution of better than 0.5 mm at a sampling interval of 150 μs. The position data are again fed back to the scanning magnets, so that any deviation of the measured from the desired beam position is immediately corrected for at the next scan point.

The time resolution of the monitoring system is designed such that it is still capable of monitoring even the large variations of intensity during the extraction cycle of the synchrotron and delivering a well defined particle number to each scan spot. It also allows for a rapid beam shut off within less than 200 ms in case of any interlock from the control system. Moreover, the total water equivalent thickness of all five chambers in the monitoring system is only about 0.7 mm.

The data of the monitoring system are also displayed in real-time on a screen, to allow a visualization of the ongoing treatment. A screenshot of this therapy online monitor is shown in Figure 5.

6. Therapy Planning

For the active beam shaping system at GSI, a research therapy planning system (TPS) was developed (Krämer et al., 2000; Jäkel et al., 2001), which fulfills the needs of the beam scanning system at GSI. While a modulator for passive beam shaping is designed to achieve a prescribed homogeneous biologically effective dose for a single field. A 3D scanning system can produce nearly arbitrary shapes of the spread out Bragg peak (SOBP). The shape of the SOBP therefore has to be optimized separately for every scan point in the irradiation field. The introduction of a 3D scanning system thus has some important consequences for the TPS:

- The beam intensity of every scan point at each energy has to be optimized separately to obtain a homogeneous biological effect.
- As the system is able to apply any complicated inhomogeneous dose distribution, the capability for intensity modulated radiotherapy with ions should be taken into account.
- All fields of a treatment plan are applied at the same day to avoid uncertainties in the resulting dose due to setup errors.
- The dose per fraction should be variable for every patient.
- The scanner control data (energy, beam position, particle number at every beam spot) have to be optimized for each field of every patient.
- An RBE model has to be implemented, that allows the calculation of a local RBE at every point in the patient depending on the spectrum of particles at this point.

6.1. Absorbed Dose Calculation

The dose calculation for active beam shaping systems relies on measured data for the depth dose curves. Instead of the measured depth dose data for the SOBPs resulting from the modulators, data for the single energies are needed. If the applied dose is variable, it is necessary to base the calculation of absorbed dose on absolute particle numbers rather than on relative values. For the calculation of absorbed dose, the integral data including all fragments are sufficient.

Before the actual dose calculation starts, the target volume is divided into slices of equal radiological depth. (Here the same empirical methods of range

calculation as for passive systems are used.) Each slice then corresponds to the range of ions at a certain energy of the accelerator. The scan positions of the raster scanner are then defined as a quadratic grid for each energy. In the last step, the particle number at each scan point is optimized iteratively until a predefined dose at each point is reached.

6.2. Biologic Modeling

To fulfill the demands of an active beam delivery on the TPS concerning the biological effectiveness, a more sophisticated biological model is needed. Such a model was developed e.g. at GSI (Scholz and Kraft, 1994, 1996; Scholz et al., 1997). Its main idea is to transfer known cell survival data for photons to ions, assuming that the difference in biological efficiency arises only from a different pattern of local dose deposition along the primary beam. It is therefore also called the local effect model (LEM).

The model takes into account the different energy deposition patterns of different ions and is thus able to model the biological effect resulting from these ions. An important prerequisite for this is, however, the detailed knowledge of the number of fragments produced as well as their energy spectrum. The calculated RBE shows a dependence on the dose level and cell type, if the underlying photon survival data for this respective cell type are known.

Another important prerequisite for the LEM model is the knowledge on the particle track structure, i.e. the radial dose distribution around the ion track, as a function of the particle charge and energy.

The LEM allows the optimization of a prescribed biologically effective dose within the target volume (Krämer et al., 2000) using the same iterative optimization algorithm as for the absorbed dose. At each iteration step, however, the RBE has to be calculated anew, as it is dependent on the particle number (or dose level). Since this includes the knowledge of the complete spectrum of fragments, the optimization is rather time consuming. Again, it has to be pointed out, that the dose dependence of the RBE demands the use of absolute dose values during optimization.

In Figure 6, the absorbed and biologically effective dose as a function of depth along the central axis in a typical treatment field for a base of skull tumor is shown. In order to achieve a homogeneous biological effect in the tumor, an optimization of the physical dose distribution (as shown in the right image) is necessary.

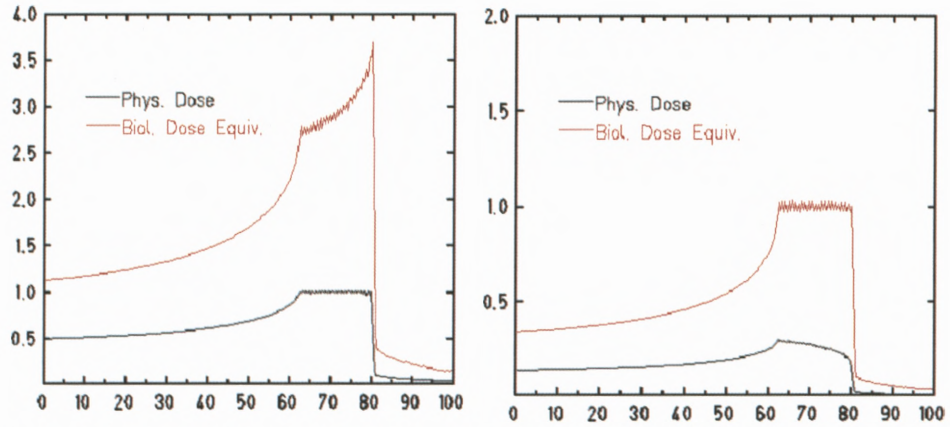

Figure 6. Absorbed and biologically effective dose resulting from a homogeneous absorbed dose (left) and from a direct optimization of a homogeneous biologically effective dose (right). Doses are given in Gy (or Gye) and depths in mm, respectively.

6.3. Secondary Neutrons

An open question arising from the nuclear fragmentation of ions is the detrimental effect of secondary neutrons. Although a number of calculations (Pshenichnov et al., 2005) and measurements (Gunzert-Marx et al., 2004) of the number of secondary neutrons produced during irradiation with carbon ions exist, it is difficult to accurately determine the effective equivalent dose due to these neutrons. This is due to a lack of knowledge on the kerma factors for the high energy secondary neutrons (neutrons up to twice the primary energy of the carbon ions are observed, i.e. up to 500 MeV neutrons for a beam of 250 MeV/μ carbon ions). It has been estimated that the dose due to secondary neutrons is less than 1% of the absorbed dose of the primary ions. The resulting risk of late effects resulting from this neutron dose is very difficult to determine. Two things should, however, clearly be noted. First, the neutrons produced are predominantly produced in forward direction, and are thus leading to irradiation of a relatively small part of the body. The biological effects will depend strongly on the direction of the beam and the type of tissues involved in that location. Second, it has been shown, that the use of an active beam delivery system leads to a production rate of neutrons, which is much lower than for a passive system (Schneider et al., 2002).

6.4. Empirical Range Calculation

In treatment planning, the selection of beam energies and the determination of ion ranges are crucial for the calculation of the delivered dose. The synchrotrons used to produce the ion beams, usually provide a very well defined and reproducible beam energy. Precision measurements of the ionization in water are used to determine the exact position and form of the Bragg curve. The accuracy of measured ion ranges in water, which can be achieved with such measurements, is better than 0.1 mm (Jäkel et al., 2001). Range calculations in tissue are then based on X-ray CT images and make use of the dependence of both, X-ray attenuation and stopping powers from the electron density. There is, however, no clear functional relation between the ion ranges and (polychromatic) X-ray attenuation since there are second order effects depending on other tissue specific quantities (the logarithmic dependence of the stopping power in the ionization potential and the strong Z-dependence of the photo-effect).

Therefore, in charged particle therapy purely empirical relations between the relative photon attenuation coefficients (called the Hounsfield units, or HU[2]) and ion ranges are used. These relations are established for phantom materials or samples of real tissues. The accuracy of the range calculation in tissue is influenced strongly by the accuracy of HU numbers. Therefore an imaging protocol for each CT scanner and treatment site has to be defined that specifies all parameters that may influence the value of the HU.

Furthermore, there are a number of effects that may disturb the quality of Hounsfield units (e.g. a contrast agent which is often used may influence the range calculation in the patient). Another unavoidable problem arises from metal artifacts. These artifacts play a role especially for tumors in the head and pelvic region, stemming from gold fillings in teeth or hip prostheses, respectively.

The described range calculation for heavy charged particles based on CT images is one of major uncertainties in ion beam therapy. Using a well defined imaging protocol for each scanner and treated anatomical site the uncertainty in the range calculation for carbon ions can be reduced to about 2–3 mm for the head and neck region. In the presence of artifacts uncertainties up to 10 mm can be observed.

[2] Given the linear absorption coefficients of a material μ and μ_W for water, the HU value is defined as $HU = 1000 \cdot (\mu - \mu_W)/\mu_W$.

7. Dosimetry

The determination of absorbed dose to water in all operating ion facilities is currently based on ionization chamber dosimetry (Kanai et al., 1999; Hartmann et al., 1999). For this purpose, commercial ionization chambers (mainly thimble type chambers) are used which are calibrated by the manufacturer in a field of Co-60 in terms of absorbed dose to water. Initially at HIMAC chambers calibrated in terms of air kerma were used, but the transition to water absorbed dose was performed recently.

This procedure is recommended also in the latest Code of Practice of the International Atomic Energy Agency, the technical report series TRS-398, which is currently the only international guideline for clinical dosimetry of ion beams (IAEA, 2000).

According to TRS-398, the absorbed dose to water at an effective point of measurement, P_{eff}, of the chamber in an ion beam is determined by:

$$D_{\text{w}}(P_{\text{eff}}) = M_{\text{corr}}\, N_{D,\text{w,Co60}}\, k_Q. \tag{1}$$

where M_{corr} is the dosimeter reading M, corrected for changes in air density, incomplete saturation, and polarity effects of the chamber. The calibration factor, N_D, w, Co60, is given by the manufacturer and k_Q is a chamber specific factor that corrects for the different beam quality of ^{12}C ions and the calibration beam quality (^{60}Co).

In TRS 398 it is suggested, that the k_Q factor is calculated theoretically as:

$$k_Q = \frac{(w_{\text{air}}/e)^{\text{C12}}}{(w_{\text{air}}/e)^{\text{Co60}}}\, \frac{\bar{s}^{\text{C12}}_{\text{w,air}}}{(\bar{L}/\rho)^{\text{Co60}}_{\text{w,air}}}\, \frac{p^{\text{C12}}}{p^{\text{Co60}}}, \tag{2}$$

which is a product of the ratios of the w values,[3] the stopping power ratios of water to air and the chamber specific perturbation factors for ^{12}C and ^{60}Co, respectively. The overall uncertainty of this determination of absorbed dose is stated to be about 3%. These three terms will be discussed briefly in the following.

7.1. Stopping Power Ratios and Ionization Potential

The calculation of the stopping power ratio has to take into account not only the fluence of primary carbon ions but also the fragments that arise from nuclear interactions and also their energy distribution. The value $s_{\text{w,air}}$ for for light ion beams in TRS-398 can be obtained as a fluence-weighted average ratio of stopping

[3] w is the mean energy required to create an electron-ion pair by a charged particle in a gas.

powers (henceforth referred to as "stopping-power ratio", not to be confused with a direct ratio of stopping powers) over the complete spectrum of primary particles and secondary particles at the reference depth:

$$s_{\mathrm{w,air}} = \frac{\sum_i \int_0^\infty \Phi_{E,i} \cdot (S_i(E)/\rho)_{\mathrm{w}} \, \mathrm{d}E}{\sum_i \int_0^\infty \Phi_{E,i} \cdot (S_i(E)/\rho)_{\mathrm{air}} \, \mathrm{d}E} \,. \tag{3}$$

Here, $(S_i(E)/\rho)$ is the mass stopping power for a particle i with energy E in water or air and $\Phi_{E,i}$ is the particle fluence differential in energy, in water for particles of type i. This method is, however, only practical if the particle fluence is well known.

In an analysis done by Hartmann et al. (1999) it was found that for energies above 10 MeV/μ the ratio of stopping powers for various light ions varies only little, and that an average constant value can be used with an uncertainty of about 2%. As a practical approach in clinical dosimetry, TRS-398 proposed to use a fixed value of 1.130.

In a recent investigation (Geithner et al., 2006), a Monte Carlo simulation of the nuclear fragmentation processes was used to analyze the dependence of the fluence averaged stopping power ratio (similar to Equation 3) on the beam energy and penetration depth. Two findings have been observed: first, the relative variation of $s_{\mathrm{w,air}}$ for various energies and depths is below 1%, except for a small region around the Bragg peak, where a maximum deviation of 4% was found. Secondly, it was found that the absolute values at high energies obtained with stopping power data from the new ICRU-73 were about 1% higher than the value recommended by TRS-398.

The reason for this discrepancy is probably a difference in the ionization potential used for various stopping power calculations. In the evaluation of the TRS-398, the ICRU-49 for proton and alpha particles and calculations by Salamon (1980) played an important role. Both data sets used I-values for water between 75 eV (ICRU 49) and 79 eV (Salamon). In the new ICRU 73, an I-value for water of 67 eV is used, which gives rise to the higher stopping power ratios. It should be noted, that a change in the I-value of 2 eV leads to a shift of the ion ranges in the order of 1 mm (Gudowska et al., 2004; Krämer et al., 2000). Therefore, a consistent analysis of stopping power data and precision range measurements would be highly desirable in order to improve the uncertainty of the dosimetry for ion beams.

7.2. W-Values for Ions

The mean energy required to produce an ion pair in air (w_{air}) is another crucial quantity in the determination of the quality correction factor. Precise measurements of the w-value are, however, difficult to perform and consequently on little experimental data for protons and ions exist (Jones, 2006; IAEA, 2000). Since the w-value again depends on the ion type and energy, in principle the same fluence averaging can be used as for the stopping power ratio (see Equation 3). Since no detailed data on the w-value for ion beams at various energies are available, TRS-398 again proposed to use a single fixed value of 34.5 eV. The uncertainty of this value was determined again from a weighting of the various sources and amounts to 1.5%. It is the second largest source of uncertainty in the dose determination for ion beams.

It is common sense that a more accurate w-value can be obtained by dosimetric measurements using an independent method, namely the water calorimetry. This method is commonly established as the primary standard for absorbed dose to water in many countries and needs only few, small corrections even for ion beams. A comparison of calorimetry with ionometry therefore might result in an indirect determination of the w-value for ion beams.

7.3. Perturbation Factors

The perturbation factor, P, for the different beam qualities includes all departures from ideal Bragg–Gray detectors, which are essentially connected to the equilibrium of secondary electrons. These are the correction for cavity effects, the displacement factor, and the effects from the chamber wall and central electrode. There are currently no data on these correction factors, which are chamber specific, in ion beams. The corresponding correction factors in photon beams are already very small. Since the secondary electrons produced in a carbon ion beam have an average energy which is lower than in the case of photon beam, the corrections are expected to be even smaller than for photons (for proton beams some estimates for the corrections exist, but the general situation is similar).

Consequently, the perturbation factors for a standard chamber in a ^{12}C ion beam, was set to unity, since no data exist that indicate a significant deviation from unity. The uncertainty of the perturbation factors in the determination of absorbed dose is stated to be 1%.

8. Dose Verification

The verification of the dose delivered to a patient by a certain treatment plan is one of the crucial points of any quality assurance system in radiotherapy. For a dynamic dose delivery, like the 3D raster scanning system, this procedure is even more important, since the dose delivery may be correct at one point in the treatment field, but deviations may appear at another point. Therefore, the dose has to be verified simultaneously at many points in the field. Such a method was introduced at the GSI, using a set of 24 small volume ionization chambers connected to a motor-driven phantom (Karger et al., 1999). It allows an efficient check of the absorbed dose in the treatment field at many points and furthermore the direct comparison with the treatment planning dose at these points. There are currently a number of ongoing developments in order to develop integrated systems with much more channels of independent ionization chambers. The aim is to get a three-dimensional sample of measured dose data in a single measurement for a certain treatment field.

At the Japanese facility HIMAC, a system was introduced (Mizota et al., 2002), that uses a 64 channel multi-layer ionization chamber with a 3×3 m^2 sensing area to measure depth dose distributions. Using the corresponding radiological depths, the dose values are transformed to the respective point in treatment planning CT. The dose distribution is then measured by sweeping the chamber through the field and reconstructing the dose on the CT-image. This procedure is certainly extremely useful for a static treatment field. For a dynamic beam application, it is not possible to move the chamber during beam application and comparable solutions have yet to be developed.

9. Conclusion

In the last decade, in 30 centers worldwide valuable clinical experience has been gained in charged particle therapy. Together with the development of new technologies especially for beam application and treatment planning there will certainly be a broader implementation of ions in clinical settings that allow for an optimal exploitation of the physical and biological potential of protons and heavy ions.

In order to allow for a successful clinical application of ion beams, a number of open questions in the field of medical physics have to be addressed. Among these are the improvements of the existing dosimetry protocols, which still lack the degree of accuracy which is current standard in conventional therapy with photon beams. Important aspects here are especially connected to the description

of the nuclear fragmentation of the heavy ions, the stopping power ratios for water to air as well as the w-values for air. Also the recommendations for I-values may have to be reconsidered in view of their importance for the stopping power and range calculations.

Another important area of physics research for particle therapy is the development of radiation detectors, which either serve as beam monitors or are used for dosimetric purposes.

References

Amaldi U. (2004): CNAO – The Italian Centre for Light-Ion Therapy. Radiother Oncol **73 Suppl 2**, S191–S201

Castro J.R., Linstadt D.E., Bahary J.-P. et al. (1994): Experience in charged particle irradiation of tumors of the skull base 1977–1992. Int J Radiat Oncol Biol Phys **29**, 647–655

Castro J.R. (1997): Clinical programs: A review of past and existing hadron protocols. In: Amaldi U., Larrson B. and Lemoigne Y. (Eds), Advances in Hadron Therapy. Elsevier Science, Amsterdam, Netherlands, pp 79–94

Geithner O., Andreo P., Sobolevsky N., Hartmann G. and Jäkel O. (2006): Calculation of stopping power ratios for carbon ion dosimetry. Phys Med Biol **51**, 2279–2292

Gudowska I., Sobolevsky N., Andreo P., Belki D. and Brahme A. (2004): Ion beam transport in tissue-like media using the Monte Carlo code SHIELD-HIT. Phys Med Biol **49**, 1933–1958

Gunzert-Marx K., Schardt D. and Simon R.S. (2004): Fast Neutrons produced by nuclear fragmentation in treatment irradiations with C12 beam. Rad Prot Dos **110, nos 1–4**, 595–600

Haberer T., Becher W., Schardt D. and Kraft G. (1993): Magnetic scanning system for heavy ion therapy. Nucl Instrum Meth A **330**, 296–305

Hartmann G.H., Jäkel O., Heeg P., Karger C.P. and Krießbach A. (1999): Determination of water absorbed dose in a carbon ion beam using thimble ionization chambers. Phys Med Biol **44**, 1193–1206

Heeg P., Eickhoff H. and Haberer T. (2004): Conception of heavy ion beam therapy at Heidelberg University (HICAT). Z Med Phys **14**, 17–24

International Atomic Energy Agency (IAEA) (Ed.) (2000): Absorbed Dose Determination in External Beam Radiotherapy. Technical Report Series No. 398, Vienna

Jäkel O. (2006): Heavy ion radiotherapy. In: Schlegel W., Bortfeld T. and Grosu A.L. (Eds), New Technologies in Radiation Oncology. Springer, Heidelberg, pp 365–378

Jäkel O., Jacob C., Schardt D., Karger C.P. and Hartmann G.H. (2001a): Relation between carbon ions ranges and X-ray CT numbers. Med Phys **28, no. 4**, 701–703

Jäkel O., Krämer M., Karger C.P. and Debus J. (2001b): Treatment planning for heavy ion radiotherapy: Clinical implementation and application. Phys Med Biol **46**, 1101–1116

Jones D. (2006): The w-value in air for proton therapy beams. Radiat Phys Chem **75**, 541–550

Kamada T., Tsujii H., Tsuji H., et al. (2002): Efficacy and safety of carbon ion radiotherapy in bone and soft tissue sarcomas. J Clin Oncol **20**, 4466–4471

Kanai T., Endo M., Minohara S., et al. (1999): Biophysical characteristics of HIMAC clinical irradiation system for heavy-ion radiation therapy. Int J Radiat Oncol Biol Phys **44**, 201–210

Karger C.P., Jäkel O., Hartmann G.H. and Heeg P. (1999): A system for three-dimensional dosimetric verification of treatment plans in intensity-modulated radiotherapy with heavy ions. Med Phys **26**: 2125–2132

Koto M., Miyamoto T., Yamamoto N., et al. (2004): Local control and recurrence of stage I non-small cell lung cancer after carbon ion radiotherapy. Radiother Oncol **71**, 147–156

Krämer M., Jäkel O., Haberer T., Kraft G., Schardt D. and Weber U. (2000): Treatment planning for heavy ion radiotherapy: Physical beam model and dose optimization. Phys Med Biol **45**, 3299–3317

Miyamoto T., Yamamoto N., Nishimura H., et al. (2003): Carbon ion radiotherapy for stage I non-small cell lung cancer. Radiother Oncol **66**, 127–140

Mizota M., Kanai T., Yusa K., et al (2002): Recontruction of biologically equivalent dose distribution on CT-image from measured physical dose distribution of therapeutic beam in water. Phys Med Biol **47**, 935–945

Pshenichnov I., Mishustin I. and Greiner W. (2005): Neutrons from fragmentation of light nuclei in tissue-like media: A study with the GEANT4 toolkit. Phys Med Biol **50**, 5493–5507

Salamon M.H. (1980): A range-energy program for relativistic heavy ions in the region $1 < E < 3000$ MeV/amu. LBL Report 10446, LBL, Berkeley

Schneider U., Agosteo S., Pedroni E. and Besserer J. (2002): Secondary neutron dose during proton therapy using spot scanning. J Rad Oncol Biol Phys **53**, 244–251

Scholz M. and Kraft G. (1994): Calculation of heavy ion inactivation probabilities based on track struckture, X-ray sensitivity and target size. *Radiat Prot Dosim* **52**, 29–33

Scholz M. and Kraft G. (1996): Track structure and the calculation of biological effects of heavy charged particles. Adv Space Res **18**, 5–14

Scholz M., Kellerer A.M., Kraft-Weyrather W. and Kraft G. (1997): Computation of cell survival in heavy ion beams for therapy – The model and its approximation. Rad Environ Biophys **36**, 59–66

Schulz-Ertner D., Haberer T., Scholz M., et al. (2002): Acute radiation-induced toxicity of heavy ion radiotherapy delivered with intensity modulated pencil beam scanning in patients with base of skull tumors. Radiother Oncol **64**, 189–195

Schulz-Ertner D., Didinger B., Nikoghosyan A., et al. (2003): Optimization of radiation therapy for locally advanced adenoid cystic carcinomas with infiltration of the skull base using photon intensity modulated radiation therapy (IMRT) and a carbon ion boost. Strahlenther Onkol **179**, 345–351

Schulz-Ertner D., Nikoghosyan A., Thilmann C., et al. (2004): Results of carbon ion radiotherapy in 152 patients. Int J Radiat Oncol Biol Phys **58**, 631–640

Sisterson J. (Ed.) (2005): Particle Newsletter 36, Harvard

Tsujii H., Mizoe J.E., Kamada T. et al. (2004): Overview of clinical experiences on carbon ion radiotherapy at NIRS. Radiother Oncol **73 Suppl 2**, S41–S49

Wilson R.R. (1946): Radiological use of fast protons. Radiology **47**, 487–491